The Berezinskii-Kosterlitz-Thouless Transition

S. Ahamed, S. Cooper, V. Pathak, and W. Reeves

Department of Physics and Astronomy, University of British Columbia, Canada.

***Abstract*— This report comprises our understanding of the Berezinskii-Kosterlitz-Thouless transition in two-dimensional systems. We start by considering the two-dimensional XY model, the physics of which maps well onto the two-dimensional Bose gases produced in cold-atom experiments. Such 2D systems are not expected to possess long-range order due to transverse fluctuations, though they exhibit quasi-long range order in finite-size systems at very low temperatures. The occurrence of the Berezinskii-Kosterlitz-Thouless transition is marked by the transition of bound vortex-antivortex pairs at low temperatures to isolated vortices and antivortices above some critical temperature. We also consider a notable experiment that explicitly shows this transition.**

I. Introduction

In 2016, David J. Thouless, F. Duncan M. Haldane, and J. Michael Kosterlitz, were awarded the Nobel Prize in Physics for "theoretical discoveries of topological phase transitions and topological phases of matter".[1] In this report we focus on the example of the Berezinskii-Kosterlitz-Thouless (BKT) transition, first exploring its theoretical origin, then its experimental realisation. This phase transition stems from the realisation that topological defects can influence the long-range order of a system.[2]

We begin by discussing the two-dimensional XY model, the theoretical regime in which the BKT transition was discovered. In particular, we investigate the possibility that a system of rotors can be arranged such that its spins form vortices. These vortices correspond to the aforementioned topological defects and [some] evidence is given for how, above some critical temperature, they may arise in a system spontaneously.

This BKT transition can be observed experimentally in trapped two-dimensional Bose gases. Since the phenomena is specific to two-dimensional systems, we discuss how the dynamics of a three-dimensional degenerate Bose gas can be constrained to just two-dimensions. The experimental methodology of detecting the phase transition is then discussed. More specifically, we focus on how two layers are imaged, and how the interference between these layers allows the change in topology to be detected.

II. The XY Model

In order to study the BKT phase transition, we will need to consider the two-dimensional XY model. The XY model is reminiscent of the Ising Model, however instead of discrete spin values we place a rotor at each site which can point in any direction in the two-dimensional plane. Such a model is described by the Hamiltonian[3]

$$H = -J\sum_{\langle i,j\rangle}\mathbf{S}_i\cdot\mathbf{S}_j \tag{1}$$

$$= -J\sum_{\langle i,j\rangle}\cos(\theta_i-\theta_j), \tag{2}$$

where θ_i corresponds to the angle of our rotor at site i. The interaction between neighbouring rotors is quantified by the constant J. This can then be expanded in powers of $(\theta_i-\theta_j)$:

$$H = -J\sum_{\langle i,j\rangle}\left[1-\frac{1}{2}(\theta_i-\theta_j)^2+O\big((\theta_i-\theta_j)^4\big)\right]. \tag{3}$$

To better quantify the structures that cause the BKT transition, it will be useful to take the continuum limit in which sites are arbitrarily close together. In this limit we will require that our rotors vary smoothly from site to site such that quantities of the order $(\theta_i-\theta_j)^4$ are negligible. This leads us to the Hamiltonian

$$H \simeq E_0+\frac{J}{2}\int d^2r\ |\nabla\theta(\mathbf{r})|^2, \tag{4}$$

where the scalar field $\theta(\mathbf{r})$ now labels the angle of the rotors at each point in the plane, and $E_0=-2JN$ is the energy of the system when all N rotors are aligned.*

A. Partition Function

We recall that the thermodynamics for a system is given by the partition function

$$Z(\beta)=\sum_n e^{-\beta E_n}=\sum_n\langle n|e^{-\beta H}|n\rangle, \tag{5}$$

where $\beta=1/k_BT$ is the inverse temperature and E_n are the energy eigenvalues of the system, $H|n\rangle=E_n|n\rangle$. This implies the second equality, where one sums over the index n labelling energy eigenstates. For the XY model, we can use the basis of "configurations" $n=\{\theta_i\}$, i.e the basis in which we specify the spin at each lattice site. This leads to

$$Z(\beta)=\sum_{\theta_i}\exp\left[J\beta\sum_{\langle i,j\rangle}cos(\theta_i-\theta_j)\right]. \tag{6}$$

Notice that we are summing over all configurations of spins; when taking the continuum limit, we have to "integrate" over all possible functions $\theta(\mathbf{r})$, as this is what replaces $\{\theta_i\}$. This is similar to the case where one replaces

*Equation 4 can be calculated explicitly by considering the action of the discrete Laplace operator in the continuum limit.

a sum over discrete momentum with an integral over continuous momentum; the result is known as the functional integral:

$$Z(\beta) \to \int D[\theta(\mathbf{r})] \exp\left[-\beta(E_0 + \frac{J}{2}\int d\mathbf{r}(\nabla\theta)^2\right]. \quad (7)$$

The exact details of the functional integral and the measure $D[\theta(\mathbf{r})]$ are not important; suffice it to say, we evaluate the Hamiltonian on every possible function $\theta(\mathbf{r})$ and sum them all up.

B. Vortices are Solutions

The integrand of this partition function is not particularly easy to deal with, so we will use perturbation theory to simplify the problem. First we define

$$\mathscr{H}[\theta] \equiv \frac{J}{2}\int d^2r\ |\nabla\theta(\mathbf{r})|^2, \quad (8)$$

and then we demand that

$$\left.\frac{\delta\mathscr{H}[\theta]}{\delta\theta(\mathbf{r})}\right|_{\theta=\theta_0} = 0. \quad (9)$$

This allows us to use a saddle point approximation, i.e. we expand our functional in terms of small fluctuations, $\delta\theta$, around functions, θ_0, that correspond to minima of $\mathscr{H}$. That is, the field configurations are approximated as $\theta(\mathbf{r}) \simeq \theta_0(\mathbf{r}) + \delta\theta(\mathbf{r})$. Using this approach, we can approximate our partition function as:

$$\begin{aligned} Z \simeq & e^{-\beta E_0}\sum_{\theta_0}\int D[\delta\theta]\exp\Bigg\{-\beta\Bigg(\mathscr{H}[\theta_0] + \\ & \frac{1}{2}\int d\mathbf{r_1}d\mathbf{r_2}\ \delta\theta(\mathbf{r_1})\left.\frac{\delta^2\mathscr{H}[\theta]}{\delta\theta(\mathbf{r_1})\delta\theta(\mathbf{r_2})}\right|_{\theta_0}\delta\theta(\mathbf{r_2})\Bigg)\Bigg\}, \end{aligned} \quad (10)$$

where we have omitted terms of the order $O(\delta\theta^3)$ and higher. We need to be careful here. For this to be a good approximation we require that the leading order contributions to Z, proportional to $H[\theta_0]$, dominate over the higher order terms that depend on $\delta\theta$ (and we sum over all minima θ_0).

Given that $H[\theta_0]$ dominates, we will find some θ_0 that solve equation 9 and use them to proceed classically. This corresponds to finding solutions of:

$$\nabla^2\theta(\mathbf{r}) = 0. \quad (11)$$

This differential equation has many solutions, the simplest of which are

$$\theta = a;\ \theta = ax + by;\ \theta = a(x^2 - y^2), \quad (12)$$

in Cartesian coordinates (x,y), $\forall a,b \in \mathbb{R}$. The first, most trivial, solution corresponds to all of our rotors pointing in the same direction - the configuration whose energy was E_0. However, there are also non-trivial solutions corresponding to topological defects such as vortices and antivortices. Figure 1 shows examples of systems including such defects. Notably, these defects cannot be reached by simple perturbations of the ground state - they correspond to non-perturbative solutions. Examples of such configurations are

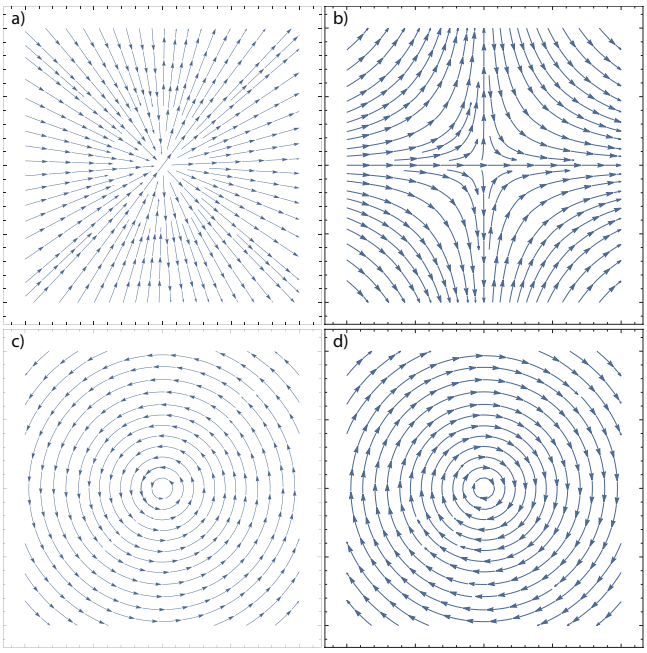

Fig. 1. Examples of systems with topological defects. a) Streamlines for the vortex θ_+. b) Streamlines for the antivortex θ_-. c) The vortex's gradient, $\nabla\theta_+$. d) The antvortex's gradient, $\nabla\theta_-$. Circulation quantifies how the vectors in c) and d) rotate when integrating along a closed path.

$$\theta_\pm = \pm\arctan\left(\frac{y-b}{x-a}\right). \quad (13)$$

θ_+ corresponds to a charge $+1$ (vortex) solution, and θ_- a charge -1 (antivortex) solution. Both θ_+ and θ_- are singular at $(x,y) = (a,b)$.

In order to quantify the (anti)vortices present in the system, we can compute a circulation integral

$$\Gamma[\theta] = \oint_\gamma \nabla\theta(\mathbf{r})\cdot d\mathbf{l} = 2\pi n. \quad (14)$$

Here n is an integer corresponding to the total charge of the vortices enclosed by the curve γ, and it is easy to check that $\Gamma[\theta_+] = 2\pi$ and $\Gamma[\theta_-] = -2\pi$. Interestingly, if one considers a curve that encloses both a vortex and an antivortex (of the same magnitude charge) then the total circulation is zero. This is well illustrated by figure 2 where we clearly see that only sites in the immediate vicinity of the vortex-antivortex pair are influenced by them; the spins far away are almost unperturbed.

These vortex solutions exhibit a rotational symmetry such that $\nabla\theta(\mathbf{r}) = \nabla\theta(r)$. Hence, we can use the circulation integral, along a radius r circle centred at the vortex's singularity, to compute $|\nabla\theta(r)|$:

$$\Gamma[\theta] = 2\pi r|\nabla\theta(r)| \quad (15)$$

$$\Rightarrow |\nabla\theta(r)| = n/r. \quad (16)$$

This result can then be substituted into the classical Hamiltonian, equation 4, to give the energy of a configuration that

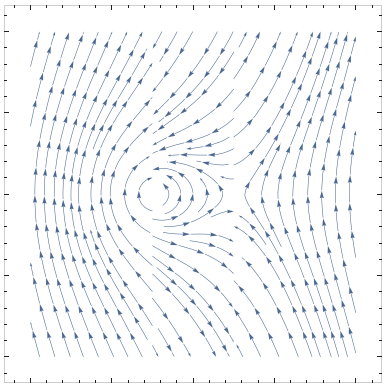

Fig. 2. A rough plot of a vortex-antivortex pair embedded in an ordered system, in which all spins were originally pointing upwards

features a single vortex:

$$E_{\text{vor}} = E_0 + \frac{J}{2}\int_a^L dr\ 2\pi r \frac{n^2}{r^2} \tag{17}$$

$$= E_0 + \pi n^2 J \ln\left(\frac{L}{a}\right). \tag{18}$$

Here, L is our system size and a is our lattice spacing, such that $N = L^2/a^2$. It's worth noting that in the limit $L \to \infty$, $a \to 0$ this quantity diverges. A similar, but less trivial, calculation can be done for a vortex-antivortex separated by some distance R. This results in an energy of the form[3]

$$E_{2\text{vor}} = E_0 + 2E_c + E_1 \ln\left(\frac{R}{a}\right), \tag{19}$$

where E_c is the energy of each individual vortex core and E_1 is some constant proportional to J. This is in agreement with the expectation that a vortex-antivortex pair will only have significant impact on the system if their separation is large.

C. Lack of long-range order in two-dimensions

We want to determine whether or not it is possible to have long range order for the XY model in an arbitrary dimension d. One way to test this is to specify the sites to be on a d-dimensional cubic lattice (with lattice spacing a and length L in each direction) and calculate the expectation value of some relevant parameter as $L \to \infty$. We choose the projection of the spins along the x direction, i.e the x magnetization, $\langle S_x \rangle = \langle \cos\theta(\mathbf{r}) \rangle$. For a cubic lattice with long range order, we expect to be able to find some non-zero expectation value, reflecting the possibility of the spins being aligned throughout the crystal. If we neglect vortex contributions (in effect allowing us to Fourier transform the field), we find[3]

$$\begin{aligned}\langle S_x \rangle &= \frac{1}{Z(\beta)} \int D[\theta(\mathbf{r})] \cos\theta(\mathbf{r}) e^{-\beta H} \\ &= \exp\left(-\frac{T}{2Ja^{2-d}} S[d] \int_{\pi/L}^{\pi/a} dk k^{d-3}\right),\end{aligned} \tag{20}$$

where $S[d]$ is the surface area of a d-dimensional sphere. We see that the integral in this expression depends strongly on the spatial dimension; as $L \to \infty$,

$$\int_{\pi/L}^{\pi/a} dk k^{d-3} = \begin{cases} \frac{L}{\pi} & d = 1 \\ \ln L/a & d = 2 \\ \frac{1}{d-2}\left(\frac{\pi}{a}\right)^{d-2} & d \geq 3. \end{cases} \tag{21}$$

We see linear divergence for $d = 1$, a logarithmic divergence for $d = 2$, and no divergence for $d \geq 3$. This leads to the conclusion that $\langle S_x \rangle = 0$ in one and two dimensions, and can posses a finite, non zero value in three dimensions. We also consider the "one body correlation function" $G_1(\mathbf{r}) \coloneqq \langle S(\mathbf{r})S(0) \rangle = \text{Re}\langle \exp[i(\theta(\mathbf{r}) - \theta(0))] \rangle$, which gives the correlation between finding the rotor at $\mathbf{r}$ at a certain angle when $\theta(0)$ is known. A similar calculation to (20) yields[3]

$$G_1(\mathbf{r}) = \begin{cases} \exp\left(-\frac{T}{2Ja} r\right) & d = 1 \\ \left(\frac{r}{L}\right)^{-\frac{T}{2\pi J}} & d = 2 \\ \exp(-CT) & d \geq 3. \end{cases} \tag{22}$$

This shows that the three and higher dimensional case is ordered, as the correlation decays to a non-zero constant. The two-dimensional case algebraically decays to 0 with r, while the one dimensional case exponentially decays to zero.

However, this algebraic decay of the correlations with distance indicates what is known as "quasi-ordering"; while in the full thermodynamic limit we lose long-range ordering, the decay of the correlation is slow enough that we can maintain some ordering for smaller system sizes. This behaviour can be observed most notably in two-dimensional Bose gases, as we will see later. Quasi-ordering is one of the reason we consider two dimensions, despite being more difficult to realize experimentally.

Recall that we have been neglecting vortices in these calculations. Vortex pairs, due to their localized effects, are expected to not alter the presence of quasi-ordering by much, while free vortices destroy it. This can be seen by considering a vortex in between 0 and $\mathbf{r}$; the presence of the vortex enforces $\theta(\mathbf{r}) \approx \theta(0) + \pi$, leading to the conclusion that if the temperature is high enough to excite free vortices, $\langle S(\mathbf{r})S(0) \rangle$ will go to zero exponentially rather than algebraically. Thus, we expect the proliferation of free vortices to correspond with the loss of quasi-ordering.

D. Spontaneous Vortex Formation

We have discussed vortices as special configurations of our system, but is it actually likely that they will arise spontaneously? Assuming we keep our system size and temperature constant, classically the viability of vortex formation is described by,

$$\Delta F = \Delta U - T\Delta S. \tag{23}$$

Where ΔF is the change in Helmholtz free energy due to adding a charge $+1$ vortex to the system. The change in internal energy from some initial configuration to some configuration with a vortex is

$$\Delta U = E_{\text{vor}}. \tag{24}$$

Here, we assume that our initial configuration is sufficiently simple, e.g. the ground state, such that vortex formation increases the internal energy by exactly the energy of one vortex. Again, assuming a sufficiently simple system then the change in entropy will be exactly the Boltzmann entropy

$$\Delta S = k_B \ln(W) \quad (25)$$
$$= k_B \ln\left(\frac{L^2}{a^2}\right). \quad (26)$$

By requiring that the vortex be centred at a lattice site, the number of microstates W is given by the total number of sites. Putting this all together we see that our change in free energy is

$$\Delta F = (\pi J - 2k_B T)\ln\left(\frac{L}{a}\right). \quad (27)$$

In the $L \to \infty$ limit this clearly diverges, however the sign of ΔF depends on the temperature:

$$\lim_{L\to\infty} \Delta F = \begin{cases} -\infty & \text{if } T > \frac{\pi J}{2k_B} \\ +\infty & \text{if } T < \frac{\pi J}{2k_B}. \end{cases} \quad (28)$$

Thus, when the temperature rises above some critical value, vortex formation will become a spontaneous process - one through which the system can reduce its free energy. This is precisely the behaviour of the BKT transition, and suggests the loss of quasi-order in the system (as in II-C). If we were not in two-dimensions then the vortex energy would not have precisely combined with the change in entropy to cause this phase transition. Whilst this is a purely classical argument, it is evidence that a BKT transition may exist.

This discussion of XY model began by discussing spins on a lattice. However, the mathematics here are simply that of scalar fields - any two-dimensional system of rotors coupled in this way, not necessarily spins, ought exhibit a similar phase transition.

III. Degenerate Bose Gases

We wish to find an example of system containing a BKT transition that can actually be observed experimentally. Consider an N-body Bose-Einstein Condensate (BEC) in three dimensions, confined by some magnetic trap. Including two particle interactions, the gas is described by the following Hamiltonian:

$$\hat{H} = \sum_i \left(\frac{\hat{\mathbf{p}}_i^2}{2m} + V_{\text{trap}}^{\text{3D}}(\hat{\mathbf{r}}_i)\right) + \sum_{i<j} U(\hat{\mathbf{r}}_i - \hat{\mathbf{r}}_j). \quad (29)$$

This Hamiltonian is simply comprised of the kinetic energy of each boson, the potential energy due to our magnetic trap, and the interaction between each particle. Experimentally one will prepare a degenerate Bose gas in which many bosons are in the approximately same quantum state (in the momentum space). Hence, using the Hartree-Fock approximation, the total wavefunction of the gas can be written in terms of the wavefunctions of individual bosons, i.e.

$$\Psi(\mathbf{r}_1, \mathbf{r}_2, \ldots, \mathbf{r}_N) = \phi(\mathbf{r}_1)\phi(\mathbf{r}_2)\ldots\phi(\mathbf{r}_N). \quad (30)$$

Using this approximation it can be shown that the mean energy of the BEC, $\langle\Psi|\hat{H}|\Psi\rangle$, is given by[†]

$$E[\phi] = \int d^3r \left(\frac{\hbar^2}{2m}|\nabla\phi(\hat{\mathbf{r}})|^2 + V_{\text{trap}}^{\text{3D}}(\hat{\mathbf{r}})|\phi(\hat{\mathbf{r}})|^2 + \frac{g}{2}|\phi(\hat{\mathbf{r}})|^4\right). \quad (31)$$

Here, we have restricted our bosons to only interact with one another via collisions, thus

$$U(\hat{\mathbf{r}} - \hat{\mathbf{r}}') = g\delta(\hat{\mathbf{r}} - \hat{\mathbf{r}}'). \quad (32)$$

This constant g is related to the three-dimensional scattering length a_{sc} of the gas by[5]

$$g = \frac{4\pi\hbar^2 a_{\text{sc}}}{m}. \quad (33)$$

A. 2D Bose Gas

We now want to achieve a two-dimensional Bose gas from our three-dimensional BEC. One way to achieve this is by adding a strong harmonic potential in the z direction, $V_{\text{harm}} = \frac{1}{2}m\omega_z^2 z^2$. With this, we can "freeze-out" one of the spatial axes by forcing every particle into the harmonic ground state along the z-axis. This allows us to write $\phi(\mathbf{r}) = \psi(x,y)\chi(z)$, with $\chi(z) \propto e^{-z^2/2a_h^2}, a_h = \sqrt{\hbar/m\omega_z}$. We can now integrate out the z component of the energy functional, yielding

$$E[\psi] = \int_A d^2r \frac{\hbar^2}{2m}|\nabla\psi|^2 + \frac{\hbar^2}{2m}\tilde{g}|\psi|^4, \quad (34)$$

where $\tilde{g} = \sqrt{8\pi}\frac{a_{sc}}{a_h}$ is the new interaction coupling, and we only integrate over the area of our trapped system. The wavefunction is best written in polar coordinates, $\psi(\mathbf{r}) = \sqrt{\rho(\mathbf{r})}e^{i\theta(\mathbf{r})}$, since the interaction energy depends only on the density $|\psi|^2 = \rho$, and for further reasons we will soon detail.

We can calculate the energy for the ground state $\psi(\mathbf{r}) = \sqrt{\rho_0}$: $E_0 = E_{in,0} = \frac{\hbar^2}{2m}\tilde{g}L^2\rho_0^2$. At low temperature, we will have excitations due to both phase and density fluctuations in the wavefunction. However, we find that $\frac{E_{in}/N}{k_B T} \gg 1$ at low temperature; this suggests that density fluctuations are greatly suppressed. Thus for the kinetic energy term, we can approximate the density as roughly constant, and we can focus on the phase fluctuations of the wavefunction $\theta : |\nabla\psi|^2 = \rho_o(\nabla\theta)^2$. This yields the exact same formula as the continuum XY model, plus a small, density dependent interaction part:

$$E[\psi] \approx E_{in,0} + \frac{\hbar^2}{2m}\rho_0 \int_A d^2r(\nabla\theta)^2 + \delta E[\delta\rho]. \quad (35)$$

We once again have saddle-points for θ corresponding to vortices. Since $\mathbf{v}(\mathbf{r}) = \frac{\hbar}{m}\nabla\theta$, a single, fixed vortex corresponds to a meta-stable (i.e a local but not global minima), unchanging fluid current around this vortex (as in figure 1c). The ability to have meta-stable currents is exactly the hallmark of a superfluid!

[†]This expression is known as the Gross-Pitaevskii Energy Functional, more information about its derivation can be found in[4].

There is one thing we must note regarding vortices and interactions We see in figure 3 that vortices correspond to zeros in the density, which certainly seems to go against the claim of the density being almost constant! In the end, however, we only care about the long distance physics, such as calculating correlation functions for relatively large r. To account for how the short distance physics (e.g vortices, interactions) affect the long distance physics, we use the heuristic of replacing the density ρ_0 with the smaller "superfluid density" ρ_s, which "absorbs" the short distance physics into it.[‡]. ρ_s essentially measures how much of the BEC is in a superfluid state; it decreases with temperature up to the BKT critical temperature, where it abruptly goes to zero.

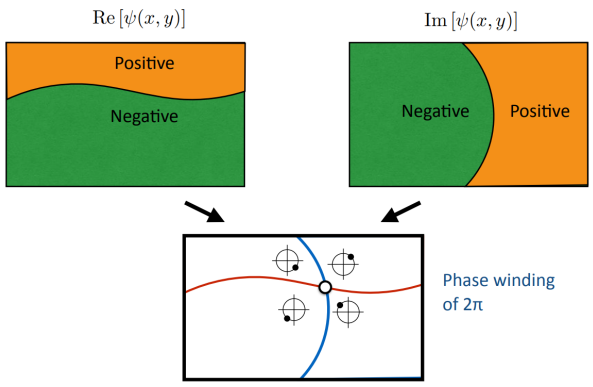

Fig. 3. Demonstrating that the location of a vortex coincides with a zero of the wavefunction, and hence a zero of the density[5].

Since equation 35 has almost the exact same functional form as equation 4, almost all the results from the XY model regarding vortices carry over, with small changes due to the interaction term. While we could calculate the actual density profile near a vortex using equation 34, and use that to calculate the interaction energy, we instead model the profile with a step function, introducing negligible changes: $\rho_{\text{vortex}}(\mathbf{r}) \approx \rho\Theta((r-r_0)-\xi)$, where $\xi = (2\tilde{g}\rho)^{-1/2}$ is the "healing length", or vortex size (determined from the proper calculation). This density can be used to calculate the change in the interaction energy for a single vortex, $\varepsilon_0 \approx \frac{\hbar^2\rho}{m}$. For a single vortex, this is negligible compared to the kinetic energy. For a vortex pair, the kinetic and interaction energy are comparable only when the vortex separation and healing length are comparable. This means the interaction terms doesn't qualitatively change the process of the BKT transition.

We now apply the previous sections results and their interpretation to the 2D BEC. We still see that vortex pairs can have small energy and so are expected at low temperature. This leads to the algebraic decay of the one body correlation function that is the signature of quasi-ordering, with an exponent $\alpha_s \propto 1/\rho_s$ that depends on the superfluid density,

$$G_1(\mathbf{r}) := \langle \psi^*(\mathbf{r})\psi(0)\rangle \approx \rho_0 e^{-\langle(\theta(r)-\theta(0))^2\rangle/2} \propto 1/r^{\alpha_s}. \quad (36)$$

Past the BKT critical temperature, free vortices proliferate and we lose quasi-ordering, leading to the exponential decay of the one body correlation function, $G_1(\mathbf{r}) \propto \exp(-r/l)$. Below the critical temperature, we expect the gas to be a superfluid, as vortex pairs can be shown to not affect a metastable circulating current, while above it we expect to lose superfluidity, as free vortices do cause fluctuations in the current as they move. This description exactly corresponds with ρ_s abruptly jumping to zero at the critical temperature, leading to a divergence in α_s.

IV. Experimental realization for the BKT transition in trapped 2D Bose gas

Experiments on liquid helium films[6], superconducting Josephson junctions[7], and 2D atomic hydrogen[8] have been used to study BKT transitions. However, only macroscopic properties of the system can be measured in such experiments. This is in contrast with various atomic physics experiments that offer access to the underlying microscopic phenomena. Moreover, experiments involving matter-wave interference allows the direct detection and visualization of the proliferation of free vortices discussed previously. In this section, we describe experimental studies of BKT transitions in two-dimensional atomic systems such as those discussed in (§ III). We discuss the results of the first such implementation by Hadzibabic et. al.[9] which has proven to be a motivation for further studies on superfluidity of Bose gases.[10].

A. *Creation of the cold two-dimensional atomic gas*

First, a degenerate cold three-dimensional cloud of atoms is produced using a Doppler cooling technique with the help of a magneto-optical trap (MOT), which basically employs a clever Zeeman shifting trick to kick the atoms to the centre of the trap[11]. The gas produced through this technique has temperature in the range of microkelvin. Further, techniques such as evaporative cooling help in bringing the temperature of the gas down to a few tens of nanokelvins. After this, a 1D optical lattice is created by standing waves using a laser along the z-axis. The atoms are coupled with the gradient of the optical lattice potential and therefore accumulate at the maxima or minima of the potential. Depending on the difference between the laser frequency and the atomic resonance frequency, the atoms accumulate at the nodes or antinodes of the standing wave. This yields an implementation of the procedure mentioned in (§ III-A), allowing for the creation of multiple strong harmonic potentials in the z-axis that compresses the gas into two-dimensional layers, as shown in figure 4.

The experiment studied here[9] uses a 3D degenerate ^{87}Rb gas subjected to 1D optical lattice potential with period $d = 3\mu$m. The lattice potential is ramped up slowly over 500ms and the resulting 2D clouds are allowed to reach thermal equilibrium for another 200ms. The potential barrier between

[‡]The technical procedure for this is known as "renormalization group flow", in which one "integrates out" the short distance degrees of freedom. However, going into the details of this procedure will take much longer than a short report!

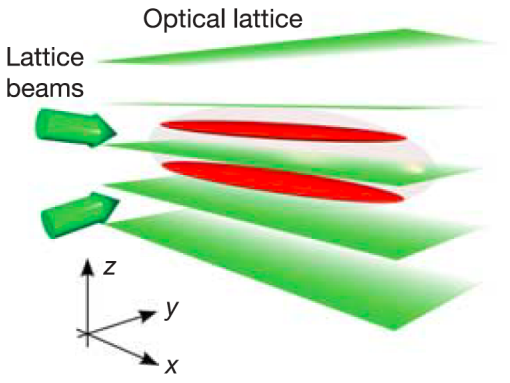

Fig. 4. A periodic optical lattice potential in the z direction created by two 532 nm laser beams intersecting at a small angle split the 3D degenerate Bose gas into two 2D planar systems.[9].

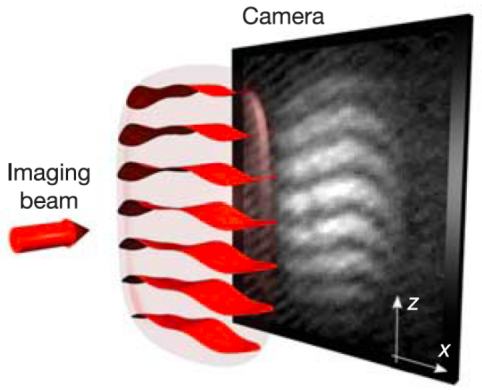

Fig. 5. The imaging of the interference pattern onto a CCD camera using the absorption of a resonant probe laser. The waviness of the interference fringes contains information about the phase patterns in the two planar systems.[9]

the planes is sufficiently large ($V_0/h = 50$ kHz) so that the tunneling between the two layers is negligible. The x and y lengths of the strips are 120 μm and 10 μm respectively. The corresponding chemical potential and healing lengths are $\mu/h = 1.7$ kHz and $\xi = 0.2\mu$m respectively.

B. Observation and interpretation of the interference pattern

After the 2D layers are obtained, the confining potential is abruptly switched off. This results in the interference of matter waves as the two clouds expand perpendicular to the x-y plane. As discussed below, imaging these interference pattern helps us detect non-trivial BKT physics taking place in these atomic two-dimensional systems. In the absorption imaging technique, a laser beam is tuned close to resonance with an atomic transition. This probe laser beam passes through the cloud and creates a shadow which is captured using a camera as shown in figure 5. A detailed description of measurement of density and momentum distribution of the atomic clouds can be found in Appendix A.

As in (§ III-A), the wavefunctions for the 2D clouds in the planes (a,b) are given by $\psi_{a,b}(x,y) = \sqrt{\rho_{a,b}}e^{i\theta_{a,b}}$. When these clouds interfere, the interference pattern depends on the relative phase $\theta_a - \theta_b$ that corresponds to the position of the fringes on the camera along the z-axis. These interference patterns can be observed by imaging along the x-z plane using a probe laser along y-axis after allowing the gases to expand for a sufficient amount of time (20 ms here). The interference signal $\rho(r)$ at position r is given by

$$\rho(r) = |\psi_a|^2 + |\psi_b|^2 + \left(\psi_a\psi_b^\star e^{i2\pi z/D_z} + c.c.\right), \tag{37}$$

where $D_z = ht/md_z$ is the period of the interference fringes and d_z is the z-axis separation between the layers. The local contrast of the interference fringes is denoted by $C(r) = \psi_a(r)\psi_b^\star(r)$. Hence, the correlation function can be calculated as

$$\begin{aligned}\langle C(r)C^\star(r')\rangle &= \langle \psi_a(r)\psi_b^\star(r)\psi_a^\star(r')\psi_b(r')\rangle \\ &= \langle \psi_a(r)\psi_a^\star(r')\rangle\langle \psi_b^\star(r)\psi_b(r')\rangle \\ &= |G_1(r,r')|^2,\end{aligned} \tag{38}$$

which gives the one-body correlation function. Since the interference image is produced in the x-z plane, it depends on the average of the density in the y direction, allowing one to obtain the y-averaged local contrast $c(x)$ through experimental fitting.

Further analysis is done by further integrating the y-averaged contrast $c(x)$ over various lengths L_x along the x-axis. With the assumption that $L_x >> L_y$, the mean value of the resulting contrast C^2, for a truly uniform system, should behave as

$$\langle C^2(L_x)\rangle \sim \frac{1}{L_x}\int_0^{L_x} dx(G_1(x,0))^2 \propto \left(\frac{1}{L_x}\right)^{2\alpha}. \tag{39}$$

For a system with true long-range order, G_1 would be constant and the interference fringes would be perfectly straight. This corresponds to the case where $\alpha = 0$, i.e., no decay of the contrast upon integration. On the other hand, if G_1 decays exponentially on a length scale much shorter than L_x (similar to the case for ideal gases and other non-ordered systems) the above integral is independent of L_x. This corresponds to the case of setting $\alpha = 1/2$, which amounts to adding up local interference fringes with random phases. For the algebraic decay found in a quasi-ordered system, an intermediate α is expected. Since the system is not truly uniform, a modified integrated contrast $\tilde{C}(L_x)$ is taken, which takes into account the non-uniformity.

The different temperature regimes for the 2D gas can be accessed by varying the final radio frequency $\nu_{\rm rf}$ used in the evaporative cooling of the 3D gas. The temperature $T \propto \Delta\nu = \nu_{\rm rf} - \nu_{\rm rf}^{\rm min}$, where $\nu_{\rm rf}^{\rm min}$ is the final radio frequency that would completely empty the trap. As a result, the temperature dependence of the average y-averaged local contrast $c_0 = \langle c(0)\rangle$ at the centre of the interference pattern can be obtained.

Figure 6 shows the fitted values of the exponent α in the different temperature regimes. At higher temperatures (corresponding to lower values of c_0, up to about 0.13), α is

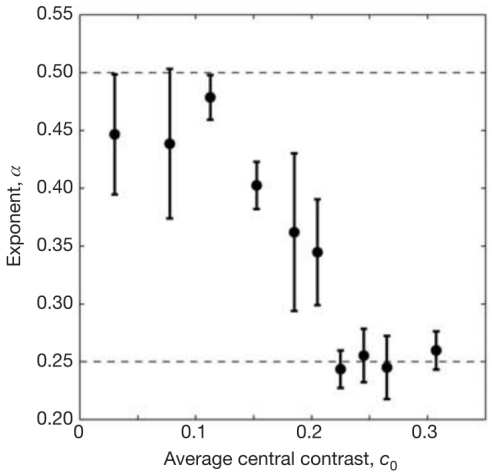

Fig. 6. Decay exponent α as a function of c_0. The dashed lines are the theoretically predicted values of α above and below the BKT transition in uniform systems.

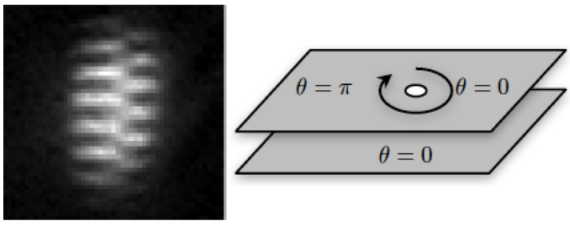

Fig. 7. The sharp dislocation in interference pattern due to vortex formation which leads to relative phase jump by π.

close to 0.5 and fairly constant, indicating a disordered system. Upon reducing the temperature (which corresponds to increasing c_0), α falls to about 0.25, indicating the presence of quasi-ordering. In the context of atomic interferometry with uniform 2D Bose gases, this sudden drop in the value of α from 0.5 to 0.25 corresponds to the 'universal jump in superfluid density'. As a result, we see a transition between two different regimes at high and low temperatures.

The merit of this experiment is that it allows for the direct visualization of vortices. If a free vortex is present in one of the interfering clouds, the relative phase $\theta_a - \theta_b$ suddenly jumps by π at the position of the vortex. Therefore, the vortex appears as a sharp dislocation in the interference pattern (provided the phase of the other cloud varies smoothly across the same region) as shown in figure 7. The vortex-antivortex pairs at much lower temperatures are not observable in the interference fringes since they create infinitesimal phase slips in the interference pattern. The probability of occurrence of these dislocations increases with increasing temperature up to the BKT critical temperature. This increase in waviness of the smooth interference pattern is shown in figure 8. Beyond the critical temperature, the interference pattern vanishes due to large phase fluctuations.

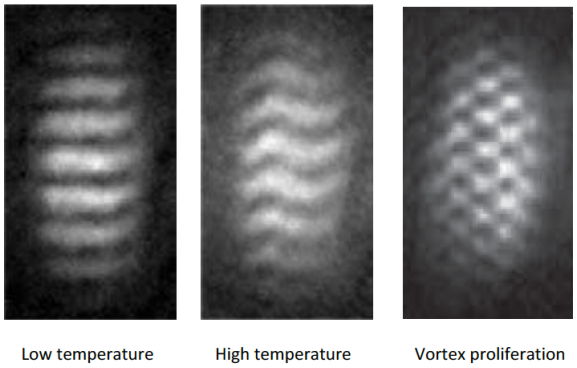

Fig. 8. Probing the coherence of 2D atomic gases using matter-wave heterodyning at different temperatures. At low temperatures, the vortex-antivortex pairs are bound together and the interference patterns are perfectly straight. At intermediate temperatures, there is a possibility of exciting a vortex which leads to sharp dislocations in the fringe pattern. There is a proliferation of free vortices at higher temperatures.

V. Conclusion

Two-dimensional systems cannot undergo conventional phase transitions associated with spontaneous symmetry breaking. In such systems, at higher temperatures, there is an exponential decay of a so-called correlation function implying that there is no long range order present. However, at low temperatures, there can be quasi-long range order in two-dimensional systems. This transition from the high-temperature disordered phase to this low-temperature quasi-ordered phase is the Berezinskii-Kosterlitz-Thouless transition. In this report, we motivated the understanding of BKT transitions by starting with the XY model and discussion of quasi-long range order in 2D systems. We discussed the role of topologically non-trivial but stable configurations called vortices in such transitions. Out of the numerous experimental implementations of this theory, we focused on experiments that involve observing these transitions in two-dimensional atomic gases. These experiments support the notion of proliferation of free vortices as the microscopic mechanism destroying the quasi-long-range coherence in 2D systems. This is directly observed in the abrupt phase shifts in the matter wave interference of two 2D atomic layers of ^{87}Rb as implemented by Hadzibabic et. al.[9]. In recent years, this has also led to direct proof of superfluid character of 2D trapped Bose gases[10].

References

[1] *The Nobel Prize in Physics 2016*. Accessed: Nov., 2018. URL: https://www.nobelprize.org/prizes/physics/2016/summary/.

[2] J. M. Kosterlitz and D. J. Thouless. "Ordering, metastability and phase transitions in two-dimensional systems". In: *Journal of Physics C: Solid State Physics* 6.7 (1973), p. 1181.

[3] H. Jeldtoft Jensen. *The Kosterlitz-Thouless Transition*. Accessed: Nov., 2018. URL: https://www.mit.edu/~levitov/8.334/notes/XYnotes1.pdf.

[4] E. H. Lieb, R. Seiringer, and J. Yngvason. "Bosons in a trap: A rigorous derivation of the Gross-Pitaevskii energy functional". In: 61.4, 043602 (Apr. 2000), p. 043602. DOI: 10.1103/PhysRevA.61.043602. eprint: math-ph/9908027.

[5] J. Dalibard. *Exploring Berezinskii-Kosterlitz-Thouless physics with cold gases*. http://www.phys.ens.fr/~dalibard/Trieste_Dalibard_1.pdf, http://www.phys.ens.fr/~dalibard/Trieste_Dalibard_2.pdf, 2018. Talks at KITP. 2018.

[6] D. J. Bishop and J. D. Reppy. "Study of the Superfluid Transition in Two-Dimensional ^{4}He Films". In: *Phys. Rev. Lett.* 40 (26 June 1978), pp. 1727–1730. DOI: 10.1103/PhysRevLett.40.1727. URL: https://link.aps.org/doi/10.1103/PhysRevLett.40.1727.

[7] D. J. Resnick et al. "Kosterlitz-Thouless Transition in Proximity-Coupled Superconducting Arrays". In: *Phys. Rev. Lett.* 47 (21 Nov. 1981), pp. 1542–1545. DOI: 10.1103/PhysRevLett.47.1542. URL: https://link.aps.org/doi/10.1103/PhysRevLett.47.1542.

[8] A. I. Safonov et al. "Observation of Quasicondensate in Two-Dimensional Atomic Hydrogen". In: *Phys. Rev. Lett.* 81 (21 Nov. 1998), pp. 4545–4548. DOI: 10.1103/PhysRevLett.81.4545. URL: https://link.aps.org/doi/10.1103/PhysRevLett.81.4545.

[9] Z. Hadzibabic et al. "Berezinskii-Kosterlitz-Thouless crossover in a trapped atomic gas". In: 441.June (2006), pp. 5–8. DOI: 10.1038/nature04851.

[10] R. Desbuquois et al. "Superfluid behaviour of a two-dimensional Bose gas". In: *Nature Physics* 8.9 (2012), pp. 645–648. ISSN: 1745-2473. DOI: 10.1038/nphys2378. URL: http://dx.doi.org/10.1038/nphys2378.

[11] I. Bloch. "Many-body Physics with Ultracold Gases". In: 80.September (2008). DOI: 10.1103/RevModPhys.80.885.

APPENDIX

A. Measurement of density and momentum distribution

In the absorption imaging technique, a laser beam is tuned close to resonance with an atomic transition. This probe laser beam passes through the cloud and creates a shadow which is captured using a camera. The interpretation of the observed atomic density distribution through this technique depends on the conditions before the imaging actually takes place. If absorptive imaging is conducted along z direction (which is perpendicular to the plane of the gas), an image of the 2D trapped atomic cloud is obtained. This depicts the (average) equilibrium density distribution of the trapped atomic gas. The spatial variation of average density is used to calculate the compressibility of the gas which, in turn, is used to deduce whether the gas is fluctuating or has suppressed density fluctuations (such as in this experiment). When the confining potential is switched off, all the interaction energy is taken out of the system without affecting in-plane momentum distribution. Subsequently, the evolution of density distribution corresponds to the free expansion of an ideal gas. In the time of flight imaging technique, the cloud is released from the trap before the image is taken. Due to free expansion, the cloud becomes larger than the initial trap depth. The image of density distribution in this case represents the momentum distribution. A sharp peak in the momentum distribution provides evidence of a BKT transition. This is because the momentum distribution is the Fourier transform of the correlation function g_1 and a significant condensed fraction with phase ordering over a large fraction of the trapped cloud gives rise to a sharp peak in the momentum distribution.